



Published in final edited form as:

Gene Ther. 2014 October ; 21(10): 913–920. doi:10.1038/gt.2014.65.

## Differential targeting of feline photoreceptors by recombinant adeno-associated viral vectors: implications for preclinical gene therapy trials

AL Minella<sup>1</sup>, FM Mowat<sup>1</sup>, KL Willett<sup>2</sup>, D Sledge<sup>3</sup>, JT Bartoe<sup>1</sup>, J Bennett<sup>2</sup>, and SM Petersen-Jones<sup>1</sup>

<sup>1</sup>Small Animal Clinical Sciences, Michigan State University, East Lansing, MI, USA

<sup>2</sup>F M Kirby Center for Molecular Ophthalmology, Scheie Eye Institute, University of Pennsylvania, Philadelphia, PA, USA

<sup>3</sup>Diagnostic Center for Population and Animal Health, Michigan State University, Lansing, MI, USA

### Abstract

The cat is emerging as a promising large animal model for preclinical testing of retinal dystrophy therapies, for example, by gene therapy. However, there is a paucity of studies investigating viral vector gene transfer to the feline retina. We therefore sought to study the tropism of recombinant adeno-associated viral (rAAV) vectors for the feline outer retina. We delivered four rAAV serotypes: rAAV2/2, rAAV2/5, rAAV2/8 and rAAV2/9, each expressing green fluorescent protein (GFP) under the control of a cytomegalovirus promoter, to the subretinal space in cats and, for comparison, mice. Cats were monitored for gene expression by *in vivo* imaging and cellular tropism was determined using immunohistochemistry. In cats, rAAV2/2, rAAV2/8 and rAAV2/9 vectors induced faster and stronger GFP expression than rAAV2/5 and all vectors transduced the retinal pigment epithelium (RPE) and photoreceptors. Unlike in mice, cone photoreceptors in the cat retina were more efficiently transduced than rod photoreceptors. In mice, rAAV2/2 only transduced the RPE whereas the other vectors also transduced rods and cones. These results highlight species differences in cellular tropism of rAAV vectors in the outer retina. We conclude that rAAV serotypes are suitable for use for retinal gene therapy in feline models, particularly when cone photoreceptors are the target cell.

### INTRODUCTION

Leber Congenital Amaurosis (LCA) is a group of hereditary retinal dystrophies with an estimated incidence of 1 in 81 000 that is characterized by early-onset vision loss.<sup>1</sup> With the recent findings that causative mutations for two feline retinal dystrophies are in genes

Correspondence: Professor SM Petersen-Jones, Michigan State University, College of Veterinary Medicine, 736 Wilson Road, D-208, East Lansing, MI 48824, USA. peter315@cvm.msu.edu.

#### CONFLICT OF INTEREST

The authors declare no conflict of interest.

Supplementary Information accompanies this paper on Gene Therapy website (<http://www.nature.com/gt>)

responsible for LCA, the cat has become a promising large animal model for preclinical testing of therapies.<sup>2,3</sup> The rod-cone dysplasia (*Rdy*) cat has a mutation in the cone rod homeobox gene (*Crx*) resulting in a severe, early-onset, dominant cone-rod dystrophy (the initial description of this as a rod-cone dystrophy was subsequently corrected<sup>3</sup>), mirroring the severe LCA<sup>CRX</sup>.<sup>4</sup> The retinal degeneration Abyssinian cat (*RdAc*) has a mutation in the centrosomal protein of 290 kDa (*Cep290*) and is a model for recessive non-syndromic *CEP290* retinopathy.<sup>2</sup> Studies to develop gene therapy vectors applicable for LCA<sup>CRX</sup> and LCA<sup>CEP290</sup> are underway and these cat models offer the opportunity to test promising approaches in a large animal model.

The feline eye and vision have been extensively studied by retinal physiologists, thus laying the groundwork for the use of this species in therapeutic studies. The similarity in size of the feline and human globe, coupled with the presence of an area centralis and visual streak with similarities to the human macula (namely higher numbers of cones and a greater density of photoreceptors)<sup>5</sup> offers advantages over rodent models for preclinical therapy testing. Canine spontaneous retinal dystrophy models, which offer similar advantages, have already proven invaluable for proof-of-concept gene therapy trials.<sup>6,7</sup> The aforementioned feline models, along with other spontaneous models currently being characterized (Rah *et al.*,<sup>8</sup> L Lyons personal communication 2013, and SM Petersen-Jones, unpublished results), show promise for this purpose.

Recombinant adeno-associated viral (rAAV) constructs have become the vectors of choice for retinal gene therapy.<sup>9</sup> However, there is limited information about the use of rAAV vectors in the feline retina. Successful gene therapy of feline mucopolysaccharidosis VI using an rAAV2 vector delivered subretinally has been reported and required transduction of the feline retinal pigment epithelium.<sup>10</sup> Only one study has been published investigating rAAV transduction of feline photoreceptor cells (the target for both LCA<sup>CRX</sup> and LCA<sup>CEP290</sup> therapy), which showed transduction of both rods and cones in two eyes injected subretinally with an rAAV2 construct.<sup>11</sup>

The purpose of the current study was to test a variety of rAAV vector serotypes delivered by subretinal injection for their potential use in preclinical retinal gene therapy trials in feline LCA models.

## RESULTS AND DISCUSSION

Subretinal injections of rAAV vectors, all at the same dose ( $1 \times 10^{11}$ vg) and all expressing green fluorescent protein (GFP), were performed on 20 feline eyes (10 cats) (Table 1). During injections, the feline retina did not detach as readily as has been our experience in the dog, and the resistance to expanding the detachment resulted in some back-flow of vector into the vitreous. Post-injection inflammation in 17 of 20 eyes was minimal consisting of trace to 1+ aqueous flare (on a scale of 1–4) during the first few days following the procedure, but this was transient and required no treatment. The retinal detachments resolved over this period. However, three eyes were excluded from the study because of the development of procedure-related intraocular inflammation (Table 1). The same vector

constructs were also injected subretinally in mouse eyes for comparison. There were no adverse complications in these eyes.

### ***In vivo* GFP expression in cat eyes**

Green fluorescence (indicative of GFP expression) was detected by *in vivo* imaging earliest in injected retinal regions of rAAV2/8 and 2/9 injected eyes, evident between 1 and 3 days, and 2 and 3 days post injection, respectively. Fluorescence in rAAV2/2- and 2/5-injected eyes developed slightly later (Table 1). Fluorescence appeared noticeably brighter in eyes injected with rAAV2/2, 2/8 and 2/9 compared with rAAV2/5-injected eyes, although this difference was not quantified. The stronger GFP expression in rAAV2/8 eyes compared with rAAV2/5 is consistent with previous reports in mice.<sup>12–14</sup> In two out of three rAAV2/2-injected eyes, evidence of posterior segment inflammation was noted (first detectable at 13–18 days post injection) and was followed by a progressive loss of GFP fluorescence, noted as decreased GFP signal on fluorescent photography (Figure 1). This decreased signal is similar to the signal decrease noted in the primate retina injected subretinally with the rAAV2-GFP construct, in which fluorescence disappeared over time; however, the kinetics of signal reduction was slower in the primate retina than we note here in the feline retina.<sup>15</sup> Fluorescence was maintained in the remaining eyes for the study duration. The onset of expression in the rAAV2/2 eyes was faster than has been reported in other species, where up to 4 weeks may be required for expression.<sup>15,16</sup>

In one rAAV2/8 eye, multiple linear, fluorescent connections between the site of the subretinal injection and the optic nerve head were noted, and most likely represented GFP within axons of the nerve fiber layer. The ciliary body in the rAAV2/2-injected eyes showed strong *in vivo* fluorescence (Figure 2).

### **Histological assessment of GFP expression**

Following euthanasia, GFP expressing cells were labeled in feline retinal sections using an anti-GFP antibody. Double labeling with markers specific for different retinal cells was performed to confirm transduced cell type. GFP expression was detected in photoreceptor cells, the retinal pigment epithelium (RPE) and some inner retinal cells for all vectors in the feline eye (Figure 3, Table 2). In mice, photoreceptors and RPE were transduced by rAAV 2/5, 2/8 and 2/9 whereas rAAV 2/2 transduced only the RPE (Figure 3).

Photoreceptor transduction was quantified by counting GFP-labeled rods and cones. For all four vectors, a significantly higher percentage of cones were transduced than rods (Table 1) and the transduced cones had noticeably brighter GFP labeling (Figure 3). rAAV2/8 transduced the highest percentage of photoreceptors, followed by rAAV2/5, rAAV2/2 and lastly rAAV2/9. The percentage of rods transduced was significantly higher in rAAV2/8-injected eyes than rAAV2/9-injected eyes (Mann–Whitney rank sum,  $P = 0.019$ ). Although quantification of photoreceptor transduction was not performed in murine retinas, those vectors that transduced photoreceptor cells subjectively appeared to have a more efficient transduction of rods than seen in cats (Figure 3).

The greater efficiency of cone transduction compared to rods in the cat retina by the rAAV serotypes used in this study was unexpected considering the findings in other species. In mice, rAAV2/2, 2/5, 2/8 and 2/9 vectors have been reported to transduce photoreceptors but with a rod predominance.<sup>12–14</sup> Similarly, it has been shown that rAAV2/2, 2/5 and 2/8 transduce canine photoreceptors, also with a rod predominance.<sup>17–21</sup> Furthermore, a study in nonhuman primates showed primarily rod transduction with rAAV2/2 and 2/8, but with some cone transduction.<sup>15</sup> Similarly, another nonhuman primate study showed strong rod transduction by rAAV2/2 and 2/8, but, similar to our findings in the feline, cone and rod transduction with rAAV2/9.<sup>22</sup> Also similar to our findings, a study investigating rAAV2/5 and 2/8 transduction showed both rod and cone transduction in the high cone/rod ratio porcine retina at comparable doses.<sup>23</sup> Studies have shown that dosage affects cone transduction with greater cone transduction at higher doses noted for rAAV2/2, rAAV2/5 and rAAV2/8.<sup>15,24</sup> The high dose we used may have contributed to the high cone transduction; however, the relatively poorer rod transduction cannot be explained by this dosage phenomenon and points to possible species differences in cone and rod receptor populations. Studies investigating expression of rAAV serotype-specific receptors on feline photoreceptors may clarify this species difference. Moreover, our findings demonstrate that rAAV2/2 transduced only RPE in murine retinas which is in contrast to other studies reporting photoreceptor transduction.<sup>14,25</sup> This could reflect a slower onset of photoreceptor versus RPE expression from rAAV2/2 in the mouse, or may, conversely, reflect expression ‘turn-off’ as was observed for this vector in some feline retinas. As mice were not euthanized until at least 55 days post injection, it is possible that the murine retina responded to rAAV2/2 similarly to the feline retina and experienced expression turn-off prior to histological evaluation.

In the cat, GFP expression in two out of three rAAV2/2 injected eyes dramatically decreased as early as 21 days post injection. Histological findings in these eyes showed subjectively thinned retinas with disruption of normal retinal architecture, most notable in the outer nuclear layer. These findings are similar to a report of rAAV2/2-injected primate retinas.<sup>15</sup> These findings were most obvious within the region of the subretinal injection; however, retinal histology outside of the subretinally injected region also showed mild retinal thinning and disorganization. Hematoxylin and eosin staining of sections of the posterior eyecup of these eyes showed a plasmacytic and lymphocytic infiltration of the retina, choroid and vitreous.

To evaluate inner retinal transduction, co-labeling for protein kinase c-alpha, calbindin, calretinin and glutamine synthetase was performed. Protein kinase c-alpha-labeled rod bipolar cells were not co-labeled for GFP, and similarly, calretinin and calbindin antibodies, both of which label certain inner retinal cells including horizontal cells, did not co-label with GFP. These results suggest that the vectors evaluated do not transduce bipolar or horizontal cells in the cat from a subretinal injection. Glutamine synthetase was used as a marker for Müller cells and showed substantial co-labeling with GFP from all vectors (Supplementary Figure 1). Glial fibrillary acidic protein was used as a marker for activated Müller cells and also showed co-labeling with GFP. Glial fibrillary acidic protein expression is increased in various retinal degenerative and inflammatory conditions, and positive labeling may therefore indicate glial cell activation associated with the therapy. Subjectively, glial

fibrillary acidic protein labeling was more extensive in eyes with brighter GFP fluorescence, suggesting that stronger GFP expression may be associated with greater activation of retinal glia<sup>24</sup> (Table 2; Supplementary Figure 1).

Transverse sections through the optic nerves showed a well-defined region of GFP labeling in all eyes injected with rAAV2/2, rAAV2/8 and rAAV2/9, but not those injected with rAAV2/5 (Figure 4). Subjectively, the GFP labeling in the optic nerve was brightest in rAAV2/8 eyes, followed by rAAV2/9, and weakest in rAAV2/2. Further investigation is required to determine if transgene expression spreads to the brain as showed in dogs and rats following subretinal injection of rAAV2/8.<sup>21,26</sup> Stromal cells in the ciliary body and iris leaflet of all eyes labeled positive for GFP (Figure 4). Exposure of these tissues to vector may have resulted from leakage from the subretinal injection site into the vitreous. There was no GFP labeling of the cornea or lens in any eyes.

**Immune response**—A neutralizing antibody assay was used to detect serum antibodies directed against the vectors in five cats; three cats that received rAAV2/2 in one eye and rAAV2/9 in the contralateral eye, and two cats that received rAAV2/5 in one eye and rAAV2/8 in the contralateral eye. Serum-neutralizing antibodies to both injected rAAV serotypes were detected in each cat (Figure 5a). The highest titer of neutralizing antibodies was to rAAV2/8, followed by rAAV2/2, rAAV2/5 and rAAV2/9. Development of neutralizing antibodies to rAAV capsids has been reported in other large animal models following injection into the immune-privileged subretinal space.<sup>23,24</sup> This highlights the importance of considering possible systemic immune reactions to rAAVs when conducting gene therapy trials. The immune response to GFP in the five cats was analyzed using an ELISA (Figure 5b). Cats injected with rAAV2/2 and rAAV2/9 had a greater titer of anti-GFP antibodies than cats injected with rAAV2/5 and rAAV2/8 (Mann–Whitney rank sum test,  $P = 0.002$ ). The inflammation and decrease in GFP expression noted in some rAAV2/2-injected eyes may be associated with the initial strong GFP expression either as a direct toxic effect or as a result of immune destruction. It is of note that GFP expression did not decrease in the contralateral rAAV2/9-treated eyes, suggesting either a direct toxic effect rather than a circulating antibody response, or that the blood–retinal barrier remained intact in the contralateral eye. Future studies analyzing the immune response in cats injected with a single vector serotype will be important to clarify these findings. Hematoxylin and eosin staining was performed to analyze inflammatory infiltration. Eighteen of 20 eyes showed at least mild lymphoplasmacytic inflammatory infiltration, with significant variation between individual eyes. Overall, infiltration was most prominent in rAAV2/9 eyes followed by rAAV2/2, then rAAV2/8 and lastly rAAV2/5 with average total infiltration scores of 9.25/12, 6.5/12, 4.7/12 and 1.3/12, respectively. Statistically, infiltration was significantly higher in rAAV2/9 eyes than rAAV2/5 eyes (Kruskal–Wallis one way analysis of variance;  $P = 0.01$ ). In all cases, the infiltration was evident across the entire retina; however, in 5/20 eyes (1 rAAV2/5, 2 rAAV2/8 and 2 rAAV2/9), the infiltration was subjectively slightly greater in the region of the bleb.

We have demonstrated that a variety of rAAV serotypes transduce feline photoreceptors. More efficient transduction of cones compared to rods differs from other species and highlights that extrapolating vector tropism between species should be made with caution.

Three of the four vectors resulted in GFP presence in ganglion cell axons within the optic nerve. Central nervous system transmission of vectors should be considered in future safety studies. The use of tissue-specific promoters may help confine expression to selected target cells, reducing or preventing off-target transgene expression.<sup>27</sup> Immune responses following rAAV gene therapy may be directed at the vector or the expressed transgene. In humans, it is estimated that up to 60% of the population has been exposed to AAV; priming of the immune system to AAVs may predispose clinical patients to even greater immune reactions than seen in preclinical animal studies.<sup>28</sup> Injecting vector through a retinotomy, as used here, may allow reflux into the vitreous. As intravitreal administration of rAAVs has been associated with an immune response that can interfere with subsequent transduction events even by the subretinal route,<sup>29,30</sup> administration route of rAAV retinal gene therapy should be carefully considered. Furthermore, vector titer is known to have a significant effect on the immune response.<sup>24</sup> The titer used here may be higher than needed for adequate therapeutic transgene expression and lower effective titers might reduce the risk of immune-related side effects. Lastly, the only immune-modulating therapy used in this study was a single subconjunctival steroid injection immediately postinjection. Additional immunosuppression may be useful to prevent inflammation and subsequent loss of transgene expression.<sup>31–33</sup>

In conclusion, the tested vectors showed preferential cone transduction making them particularly suited for therapy targeted at cone photoreceptors. Further studies testing additional vector and promoter combinations are required to identify the optimal construct for targeting both rods and cones for gene therapy trials in the *Crx* and *Cep290* mutant cat models. Further studies are also necessary to better characterize the central nervous system transmission of rAAV vectors and investigate any associated immune responses.

## MATERIALS AND METHODS

### Animals

Ten adult wild-type male domestic shorthair cats (Liberty Research, Inc., Waverly, NY, USA) and eight 3–4-week old female C57Bl6J mice (Harlan Sprague Dawley Inc., Indianapolis, IN, USA) were used. All procedures were conducted according to the ARVO Statement for the Use of Animals in Ophthalmic and Vision Research and were approved by the Michigan State University Institutional Animal Care and Use Committee.

### Production of vector

Recombinant adeno-associated virus 2/2, 2/5, 2/8 and 2/9 vectors packaged with the GFP gene driven by the cytomegalovirus promoter were produced by the University of Pennsylvania Viral Vector Core. rAAV vectors were manufactured and purified from cell lysates after triple transfection in HEK293 cells. rAAV particles were purified from cell lysates by two rounds of cesium chloride centrifugation. Vector was concentrated and desalted, using Amicon Ultra-15 centrifugal filtration devices (Millipore, Bedford, MA, USA). Glycerol was added to the concentrate to a final concentration of 5% (v/v), and aliquots were stored at –80 °C. All vector preparations were evaluated by multiple assays, including whole purity analysis by sodium dodecyl sulfate–polyacrylamide gel electrophoresis, endotoxin determination (with < 20 EU ml<sup>–1</sup> as a lot release criterion), and



by TaqMan quantitative PCR for genome copy titration. For subretinal injection, vectors were diluted to a titer of  $5 \times 10^{11}$  viral genomes per milliliter (vgml<sup>-1</sup>) in sterile balanced salt solution (Alcon Laboratories, Fort Worth, TX, USA).

### Subretinal injections

Subretinal injections in cats were performed using the technique previously described in dogs<sup>34</sup> but with the addition of a standard three-port 23-gauge vitrectomy; 200 µl of vector was injected. Six cats received rAAV2/5 in the right eye and rAAV2/8 in the left eye, and four cats received rAAV2/9 in the right eye and rAAV2/2 in the left eye. Postoperatively, 0.2 mg dexamethosone (Bimeda LC, Oakbrook, IL, USA) and 4mg methylprednisolone acetate (Depomedrol. Pfizer Animal Health, Madison, NJ, USA) were injected subconjunctivally. Approximately 2µl of vector was subretinally injected into mice using a transcleral approach as previously described.<sup>35</sup> Following injection, neomycin/bacitracin/polymyxin B ointment (Henry Schein, Melville, NY, USA) was applied twice daily for 2 days. Each vector was injected into four mouse eyes.

### Monitoring for GFP expression

Fundus photography and GFP expression monitoring was performed in cats daily for 10 days, every-other-day for 1 week, twice weekly for 1 week and once weekly until euthanasia (RetCam II. Clarity Medical Systems, Pleasanton, CA, USA). Mice were maintained for 6–8 weeks, during which time only gross ocular examinations were performed.

### Eye processing

Cats were euthanized 21–56 days and mice 55–71 days post injection. Feline globes were fixed in 4% paraformaldehyde and dissected along the limbus, dividing the anterior and posterior segments. Mouse globes were fixed in 1% paraformaldehyde. Feline anterior and posterior segments and whole mouse eyes were embedded in optimal cutting temperature gel (OCT. Sakura Finetek USA, Inc., Torrance, CA, USA) and flash frozen. Serial 14 µm (cat) and 10 µm (mouse) cryosections were prepared for immunohistochemistry.

### Immunohistochemistry

Immunohistochemistry was performed as previously described.<sup>36</sup> Antibodies are listed in Table 3. Feline sections were imaged using an Olympus FluoView 1000 Laser Scanning Confocal microscope (Olympus American Inc., Melville, NY, USA). Z-depth series were constructed using Image J software and examined using Adobe Photoshop 3.0 software (Adobe Systems Inc., Mountain View, CA, USA).<sup>37</sup> Murine sections were imaged using a Nikon Eclipse 80i microscope (Nikon instruments Inc., Melville, NY, USA) equipped with a CoolSnap ESv camera (Photometrics, Tuscon, AZ, USA).

### Cell counting

Rod and cone photoreceptors expressing GFP in cat eyes were counted. Images from three retinal sections from each injected region of each eye stained with CAR and DAPI were captured. With the GFP signal masked and cones labeled with CAR, a masked observer counted and marked 200 rod photoreceptor cell bodies. The GFP signal was then unmasked

and all marked cell bodies positive for GFP expression were counted. Non-transduced rods were not directly counted but were assessed as the number of GFP-positive rods subtracted from the total number of rods marked (200). All cones (CAR positive) across sections were counted and the number of GFP-labeled cones were recorded.

### Immune responses

To detect antibodies against rAAVs, an *in vitro* transduction assay was adapted from previous methods.<sup>38</sup> Briefly, 84-31 cells (293 HEK stably expressing Ad-E4, University of Pennsylvania Vector Core) were seeded overnight at 6000 cells per well. Half-log serial dilutions of test sera (1:3.16–1:10 000) were incubated with appropriate rAAV serotypes containing a GFP reporter at a multiplicity of infection (MOI) optimized such that ~80% of cells were transduced in control wells lacking test sera. Plates were inoculated and incubated at 37 °C under 5% CO<sub>2</sub> for 36 h and then assayed for GFP fluorescence with a Typhoon 9400 Variable Mode Imager (GE Healthcare, Piscataway, NJ, USA). Images were analyzed with Protein Array Analyzer for ImageJ<sup>39</sup> and samples are reported as neutralizing when fluorescence was < 50% of uninhibited controls. An indirect enzyme-linked immunosorbent assay (ELISA) was performed to detect anti-GFP antibodies in serum samples; 0.1 µg of recombinant purified GFP (Clontech, Palo Alto, CA, USA) was incubated overnight at 4 °C then blocked and incubated with feline test sera diluted to 1:400. Samples were then incubated with HRP-conjugated anti-feline IgG secondary antibody (Thermo Fisher Scientific, Waltham, MA, USA) diluted to 1:10 000. The plate was developed using SIGMAFAST OPD system (Sigma-Aldrich, St Louis, MO, USA). Results are presented relative to serum from an un-injected naïve cat. All samples were run in triplicate. For evaluation of inflammatory infiltration three sections of each eye was stained with hematoxylin and eosin stain and evaluated based on an objective scoring system (Table 4). Four ocular regions were designated and scored and a total infiltration score was determined for each eye by adding the four individual scores.

### Statistical analysis

All statistical analysis was conducted using SigmaPlot software (SigmaPlot 12. Systat Software Inc., San Jose, CA, USA). Normally distributed cell counting data sets (determined by Shapiro–Wilk normality test) were compared using unpaired *t*-tests. Nonparametric cell counting data sets were compared by a Mann–Whitney rank sum test. Significance was set at  $P < 0.05$ . The hematoxylin and eosin data were analyzed using Kruskal–Wallis one way analysis of variance with significance set at  $P < 0.05$ .

### Supplementary Material

Refer to Web version on PubMed Central for supplementary material.

### ACKNOWLEDGEMENTS

Funding for this study was provided by the Grousbeck Family Foundation, the Hal and Jean Glassen Memorial Foundation, the Myers Dunlap Endowment (to SMP-J) and research grants from the National Institutes of Health (8DP1EY023177 and 1R24EY019861 to JB, and T32OD011167 to Michigan State University), Foundation Fighting Blindness, and Research to Prevent Blindness. We would like to thank Janice Querubin and Lisa Allen for their assistance and animal care, and Cheryl Craft for providing the cone arrestin antibody.



## REFERENCES

1. Stone EM. Leber congenital amaurosis - a model for efficient genetic testing of heterogeneous disorders: LXIV Edward Jackson Memorial Lecture. *Am J Ophthalmol.* 2007; 144:791–811. [PubMed: 17964524]
2. Menotti-Raymond M, David VA, Schaffer AA, Stephens R, Wells D, Kumar-Singh R, et al. Mutation in CEP290 discovered for cat model of human retinal degeneration. *J Hered.* 2007; 98:211–220. [PubMed: 17507457]
3. Menotti-Raymond M, Deckman KH, David V, Myrkalo J, O'Brien SJ, Narfstrom K. Mutation discovered in a feline model of human congenital retinal blinding disease. *Invest Ophthalmol Vis Sci.* 2010; 51:2852–2859. [PubMed: 20053974]
4. Furukawa T, Morrow EM, Cepko CL. Crx a novel otx-like homeobox gene, shows photoreceptor-specific expression and regulates photoreceptor differentiation. *Cell.* 1997; 91:531–541. [PubMed: 9390562]
5. Linberg KA, Lewis GP, Shaaw C, Rex TS, Fisher SK. Distribution of S- and M-cones in normal and experimentally detached cat retina. *Journal Comp Neurol.* 2001; 430:343–356.
6. Acland GM, Aguirre GD, Ray J, Zhang Q, Aleman TS, Cideciyan AV, et al. Gene therapy restores vision in a canine model of childhood blindness. *Nat genet.* 2001; 28:92–95. [PubMed: 11326284]
7. Beltran WA, Cideciyan AV, Lewin AS, Iwabe S, Khanna H, Sumaroka A, et al. Gene therapy rescues photoreceptor blindness in dogs and paves the way for treating human X-linked retinitis pigmentosa. *Proc Natl Acad Sci USA.* 2012; 109:2132–2137. [PubMed: 22308428]
8. Rah H, Maggs DJ, Blankenship TN, Narfström K, Lyons LA. Early-onset autosomal recessive, progressive retinal atrophy in Persian cats. *Invest Ophthalmol Vis Sci.* 2005; 46:1742–1747. [PubMed: 15851577]
9. Buch PK, Bainbridge JW, Ali RR. AAV-mediated gene therapy for retinal disorders: from mouse to man. *Gene Therapy.* 2008; 15:849–857. [PubMed: 18418417]
10. Ho TT, Maguire AM, Aguirre GD, Surace EM, Anand V, Zeng Y, et al. Phenotypic rescue after adeno-associated virus-mediated delivery of 4-sulfatase to the retinal pigment epithelium of feline mucopolysaccharidosis VI. *J Gene Med.* 2002; 4:613–621. [PubMed: 12439853]
11. Bainbridge JW, Mistry A, Schlichtenbrede FC, Smith A, Broderick C, De Alwis M, et al. Stable rAAV-mediated transduction of rod and cone photoreceptors in the canine retina. *Gene Therapy.* 2003; 10:1336–1344. [PubMed: 12883530]
12. Allocca M, Mussolino C, Garcia-Hoyos M, Sanges D, Iodice C, Petrillo M, et al. Novel adeno-associated virus serotypes efficiently transduce murine photoreceptors. *J Virol.* 2007; 81:11372–11380. [PubMed: 17699581]
13. Natkunarajah M, Trittibach P, McIntosh J, Duran Y, Barker SE, Smith AJ, et al. Assessment of ocular transduction using single-stranded and self-complementary recombinant adeno-associated virus serotype 2/8. *Gene Therapy.* 2008; 15:463–467. [PubMed: 18004402]
14. Leberherz C, Maguire A, Tang W, Bennett J, Wilson JM. Novel AAV serotypes for improved ocular gene transfer. *J Gene Med.* 2008; 10:375–382. [PubMed: 18278824]
15. Vandenberghe LH, Bell P, Maguire AM, Cearley CN, Xiao R, Calcedo R, et al. Dosage thresholds for AAV2 and AAV8 photoreceptor gene therapy in monkey. *Sci Transl Med.* 2011; 3:88ra54.
16. Rabinowitz JE, Rolling F, Li C, Conrath H, Xiao W, Xiao X, et al. Cross-packaging of a single adeno-associated virus (AAV) type 2 vector genome into multiple AAV serotypes enables transduction with broad specificity. *J Virol.* 2002; 76:791–801. [PubMed: 11752169]
17. Mowat FM, Gornik KR, Dinculescu A, Boye SL, Hauswirth WW, Petersen-Jones SM, et al. Tyrosine capsid-mutant AAV vectors for gene delivery to the canine retina from a subretinal or intravitreal approach. *Gene Therapy.* 2013; 21:96–105. [PubMed: 24225638]
18. Beltran WA. The use of canine models of inherited retinal degeneration to test novel therapeutic approaches. *Vet Ophthalmol.* 2009; 12:192–204. [PubMed: 19392879]
19. Bainbridge JW, Mistry A, Schlichtenbrede FC, Smith A, Broderick C, De Alwis M, et al. Stable rAAV-mediated transduction of rod and cone photoreceptors in the canine retina. *Gene Therapy.* 2003; 10:1336–1344. [PubMed: 12883530]

20. Acland GM, Aguirre GD, Bennett J, Aleman TS, Cideciyan AV, Bennicelli J, et al. Long-term restoration of rod and cone vision by single dose rAAV-mediated gene transfer to the retina in a canine model of childhood blindness. *Mol Ther.* 2005; 12:1072–1082. [PubMed: 16226919]
21. Stieger K, Colle MA, Dubreil L, Mendes-Madeira A, Weber M, Le Meur G, et al. Subretinal delivery of recombinant AAV serotype 8 vector in dogs results in gene transfer to neurons in the brain. *Mol Ther.* 2008; 16:916–923. [PubMed: 18388922]
22. Vandenberghe LH, Bell P, Maguire AM, Xiao R, Hopkins TB, Grant R, et al. AAV9 targets cone photoreceptors in the nonhuman primate retina. *PLoS One.* 2013; 8:e53463. [PubMed: 23382846]
23. Mussolino C, della Corte M, Rossi S, Viola F, Di Vicino U, Marrocco E, et al. AAV-mediated photoreceptor transduction of the pig cone-enriched retina. *Gene Therapy.* 2011; 18:637–645. [PubMed: 21412286]
24. Beltran WA, Boye SL, Boye SE, Chiodo VA, Lewin AS, Hauswirth WW, et al. rAAV2/5 gene-targeting to rods:dose-dependent efficiency and complications associated with different promoters. *Gene Therapy.* 2010; 17:1162–1174. [PubMed: 20428215]
25. Gao G, Vandenberghe LH, Wilson JM. New recombinant serotypes of AAV vectors. *Curr Gene Ther.* 2005; 5:285–297. [PubMed: 15975006]
26. Dudus L, Anand V, Acland GM, Chen SJ, Wilson JM, Fisher KJ, et al. Persistent transgene product in retina, optic nerve and brain after intraocular injection of rAAV. *Vision Res.* 1999; 39:2545–2553. [PubMed: 10396623]
27. Mancuso K, Hendrickson AE, Connor TB Jr, Mauck MC, Kinsella JJ, Hauswirth WW, et al. Recombinant adeno-associated virus targets passenger gene expression to cones in primate retina. *J Opt Soc Am A Opt Image Sci Vis.* 2007; 24:1411–1416. [PubMed: 17429487]
28. Boutin S, Monteilhet V, Veron P, Leborgne C, Benveniste O, Montus MF, et al. Prevalence of serum IgG and neutralizing factors against adeno-associated virus (AAV) types 1, 2, 5, 6, 8, and 9 in the healthy population: implications for gene therapy using AAV vectors. *Hum Gene Ther.* 2010; 21:704–712. [PubMed: 20095819]
29. Anand V, Duffy B, Yang Z, Dejneka NS, Maguire AM, Bennett J. A deviant immune response to viral proteins and transgene product is generated on subretinal administration of adenovirus and adeno-associated virus. *Mol Ther.* 2002; 5:125–132. [PubMed: 11829519]
30. Li Q, Miller R, Han PY, Pang J, Dinculescu A, Chiodo V, et al. Intraocular route of AAV2 vector administration defines humoral immune response and therapeutic potential. *Mol Vis.* 2008; 14:1760–1769. [PubMed: 18836574]
31. Chirmule N, Xiao W, Truneh A, Schnell MA, Hughes JV, Zoltick P, et al. Humoral immunity to adeno-associated virus type 2 vectors following administration to murine and nonhuman primate muscle. *J Virol.* 2000; 74:2420–2425. [PubMed: 10666273]
32. Halbert CL, Standaert TA, Wilson CB, Miller AD. Successful readministration of adeno-associated virus vectors to the mouse lung requires transient immunosuppression during the initial exposure. *J Virol.* 1998; 72:9795–9805. [PubMed: 9811715]
33. Kay MA, Meuse L, Gown AM, Linsley P, Hollenbaugh D, Aruffo A, et al. Transient immunomodulation with anti-CD40 ligand antibody and CTLA4Ig enhances persistence and secondary adenovirus-mediated gene transfer into mouse liver. *Proc Natl Acad Sci USA.* 1997; 94:4686–4691. [PubMed: 9114052]
34. Petersen-Jones SM, Bartoe JT, Fischer AJ, Scott M, Boye SL, Chiodo V, et al. AAV retinal transduction in a large animal model species: comparison of a self-complementary AAV2/5 with a single-stranded AAV2/5 vector. *Mol Vis.* 2009; 15:1835–1842. [PubMed: 19756181]
35. Tan MH, Smith AJ, Pawlyk B, Xu X, Liu X, Bainbridge JB, et al. Gene therapy for retinitis pigmentosa and Leber congenital amaurosis caused by defects in AIPL1: effective rescue of mouse models of partial and complete Aipl1 deficiency using AAV2/2 and AAV2/8 vectors. *Hum Mol Genet.* 2009; 18:2099–2114. [PubMed: 19299492]
36. Mowat FM, Breuwer AR, Bartoe JT, Annear MJ, Zhang Z, Smith AJ, et al. RPE65 gene therapy slows cone loss in Rpe65-deficient dogs. *Gene Therapy.* 2013; 20:545–555. [PubMed: 22951453]
37. Schneider CA, Rasband WS, Eliceiri KW. NIH Image to ImageJ: 25 years of image analysis. *Nat Methods.* 2012; 9:671–675. [PubMed: 22930834]

38. Kay MA, Manno CS, Ragni MV, Larson PJ, Couto LB, McClelland A, et al. Evidence for gene transfer and expression of factor IX in haemophilia B patients treated with an AAV vector. *Nat Genet.* 2000; 24:257–261. [PubMed: 10700178]
39. Carpentier, G.; Henault, E. Protein array analyzer for ImageJ. In: Tudor, H., editor. *Proceedings of the ImageJ User and Developer Conference*. Belvaux, Luxembourg: Centre de Recherche Public; 2010. p. 238-240.
40. Li A, Zhu X, Brown B, Craft CM. Gene expression networks underlying retinoic acid-induced differentiation of human retinoblastoma cells. *Invest Ophthalmol Vis Sci.* 2003; 44:996–1007.

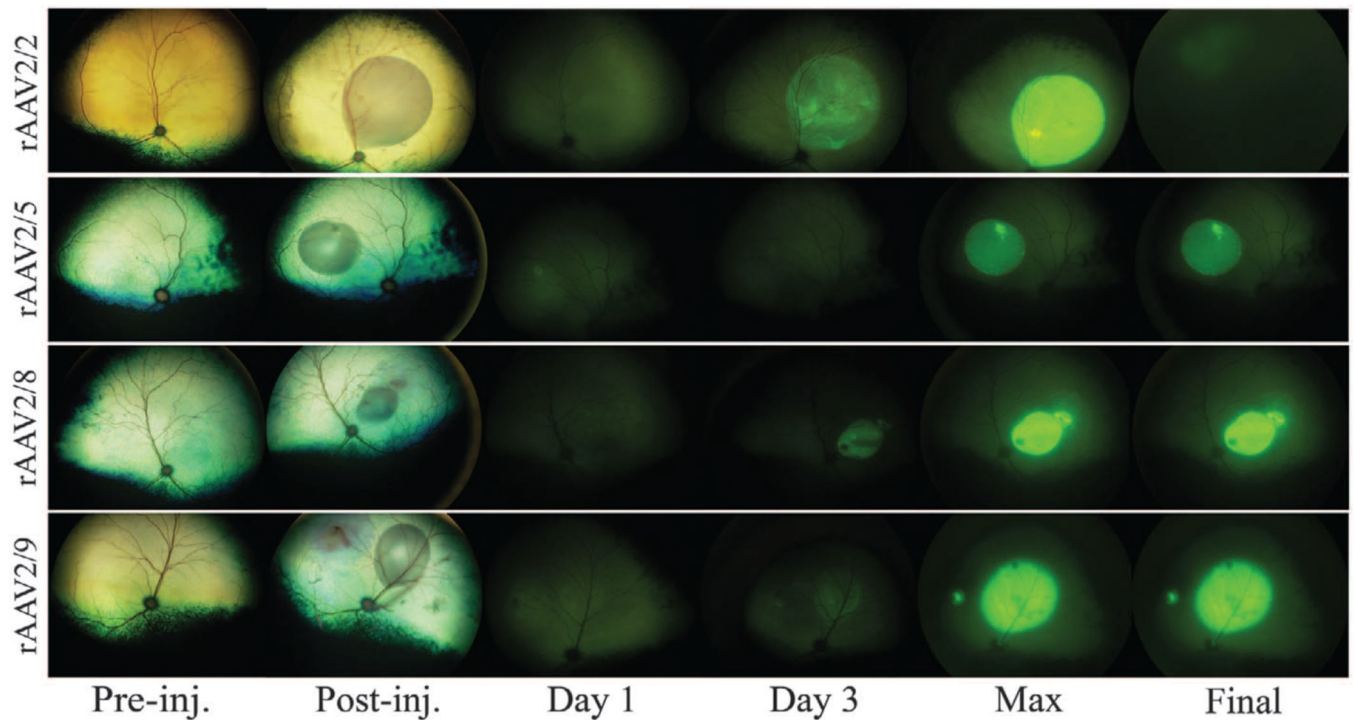


**Figure 1.**

*In vivo* transduction of the retina. Representative fundus images of cats from each vector group. Pre-injection (Pre-inj.) column shows the fundus preoperatively and post injection (Post-inj.) images show the 'bleb' created by vector subretinal injection (color images). GFP fluorescence images for the same eyes are shown in subsequent columns at day 1, day 3, maximum GFP expression (Max) and immediately prior to euthanasia (final). Maximum GFP intensity was reached by days 12 for rAAV2/2, 35 for rAAV2/5, 24 for rAAV2/8 and 28 for rAAV2/9. Note the decrease in GFP expression in the rAAV 2/2 eye.

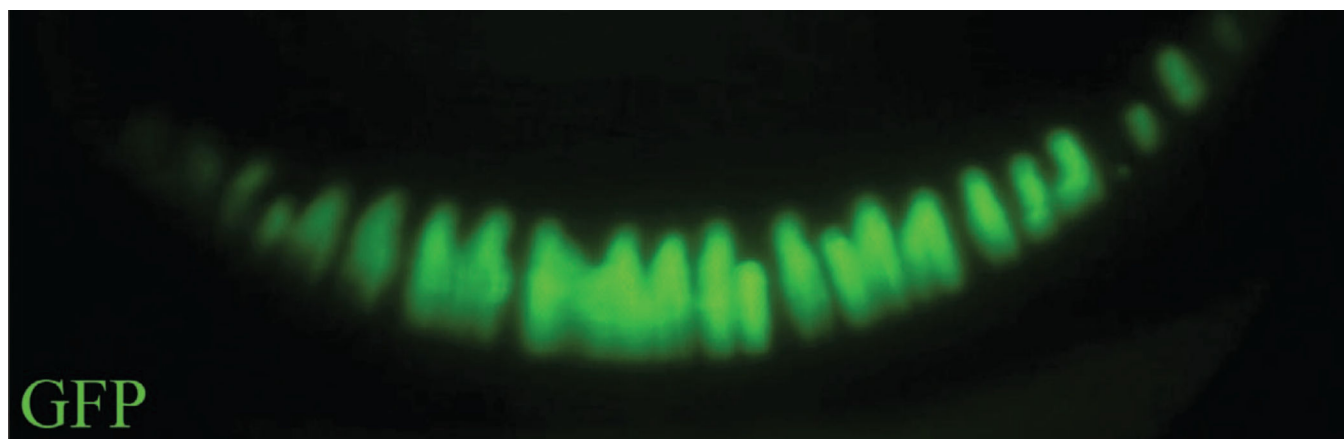


**Figure 2.**

*In vivo* expression in the ciliary body. *In vivo* wide-field fundus photograph illustrating rAAV2/2 expression in the ciliary processes. All vectors transduced the ciliary processes, but *in vivo* fluorescence was only noted in rAAV2/2-injected eyes.



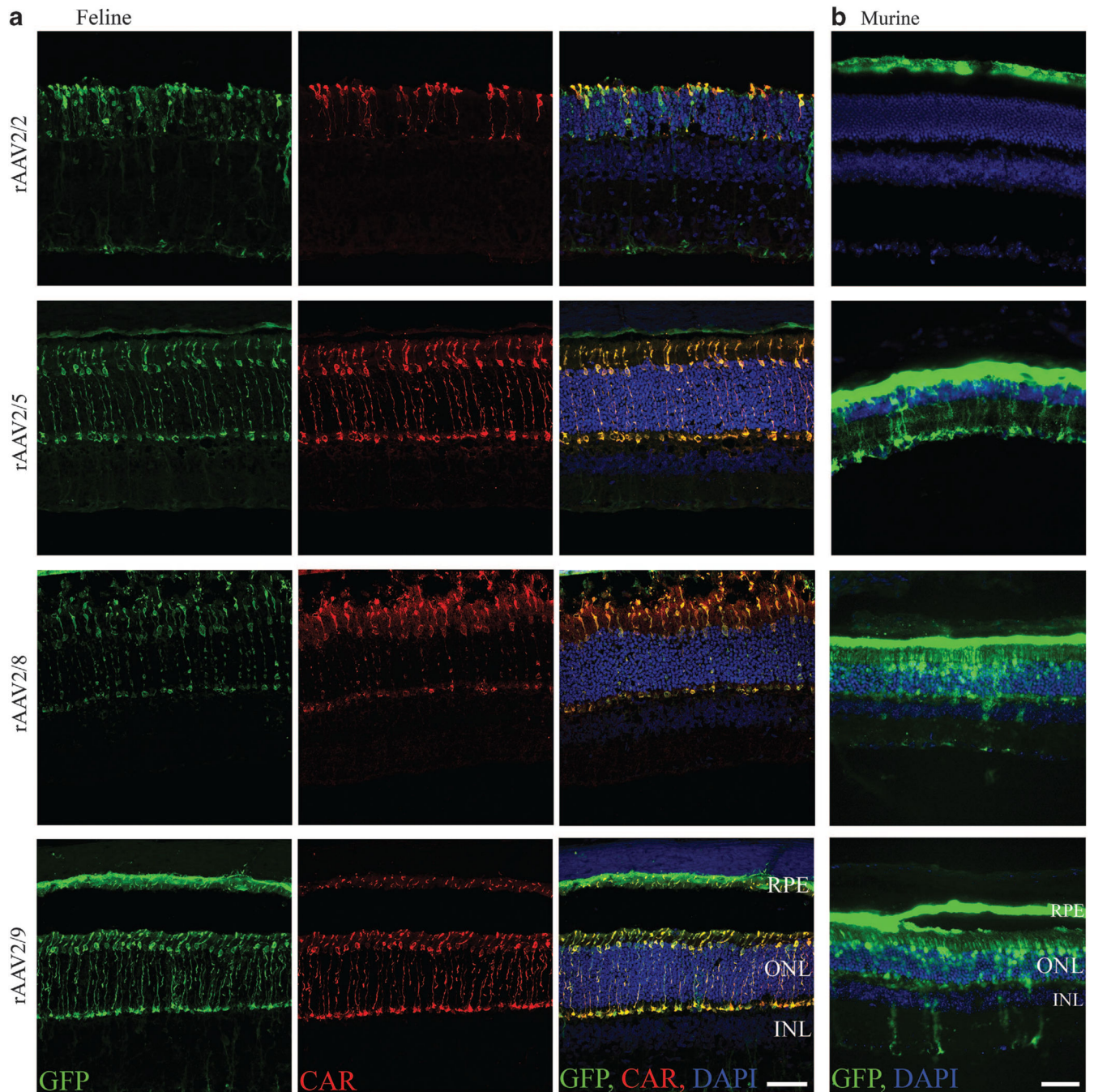


**Figure 3.**

Histological transduction of feline and murine outer retinas. **(a)** Feline retinal sections co-labeled with a GFP antibody and cone arrestin antibody show the predominance of cone transduction for each of the vectors. rAAV2/2 eyes all showed inflammation, thereby affecting section quality, as evidenced in the rAAV2/2 images. **(b)** In murine retinas, rAAV 2/5, 2/8 and 2/9 vectors transduced rods, cones and RPE, whereas rAAV 2/2 only transduced the RPE. Scale bar=50  $\mu$ m. CAR, cone arrestin labeling; DAPI, nuclear counterstain; INL, inner nuclear layer; ONL, outer nuclear layer.



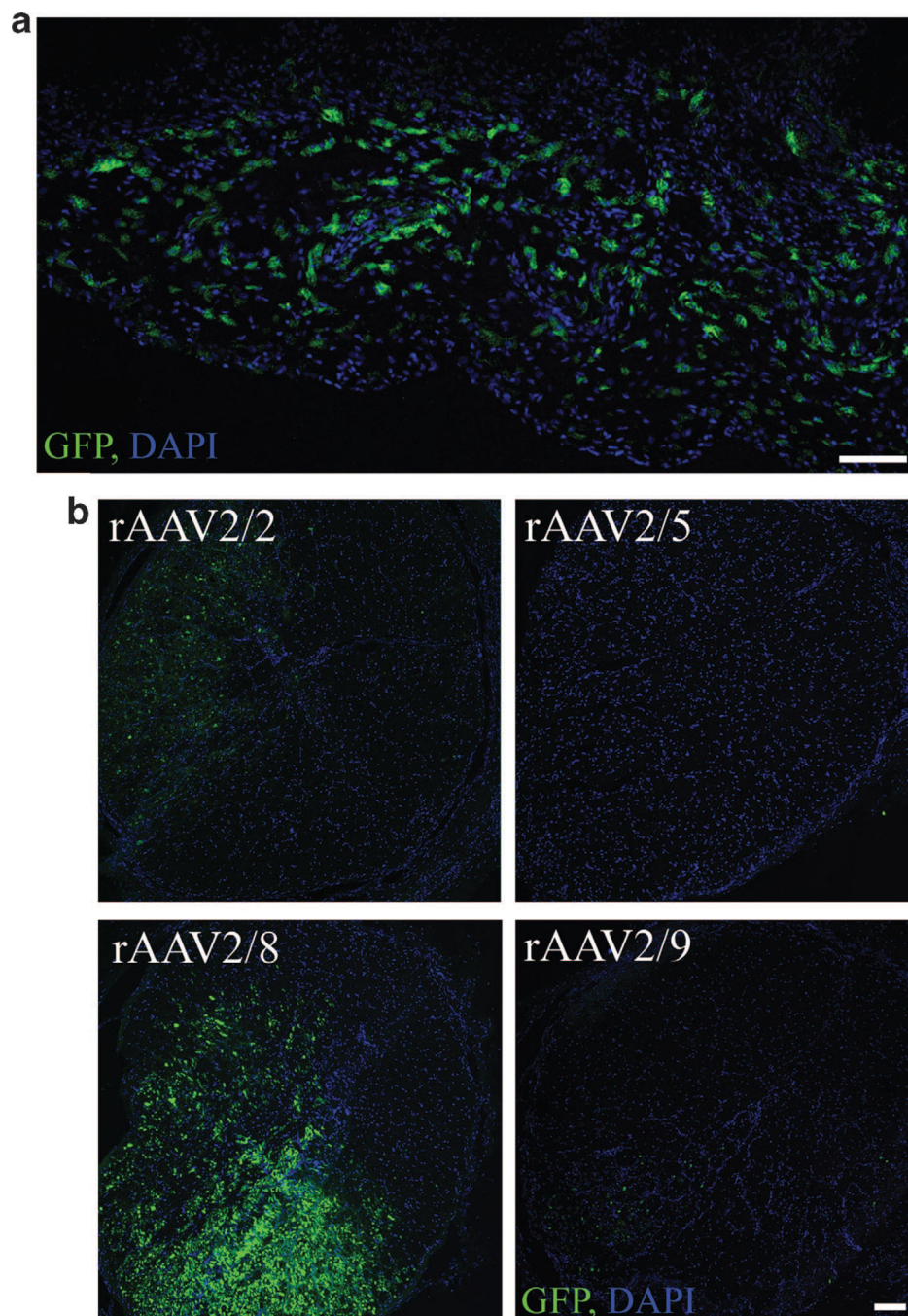


**Figure 4.**

Histological sections showing GFP expression in other parts of the feline eye. (a) Representative histological image of the ciliary body from an rAAV2/2-injected eye illustrating transduction of cells within the stroma of the ciliary processes. There were similar findings for all vector types. (b) Histological sections of optic nerve from each vector. rAAV 2/8, 2/9 and 2/2 showed transduction of the optic nerve, with 2/8 showing the strongest transduction. rAAV2/5 showed no transduction of the optic nerve. Scale bar=100  $\mu$ m.

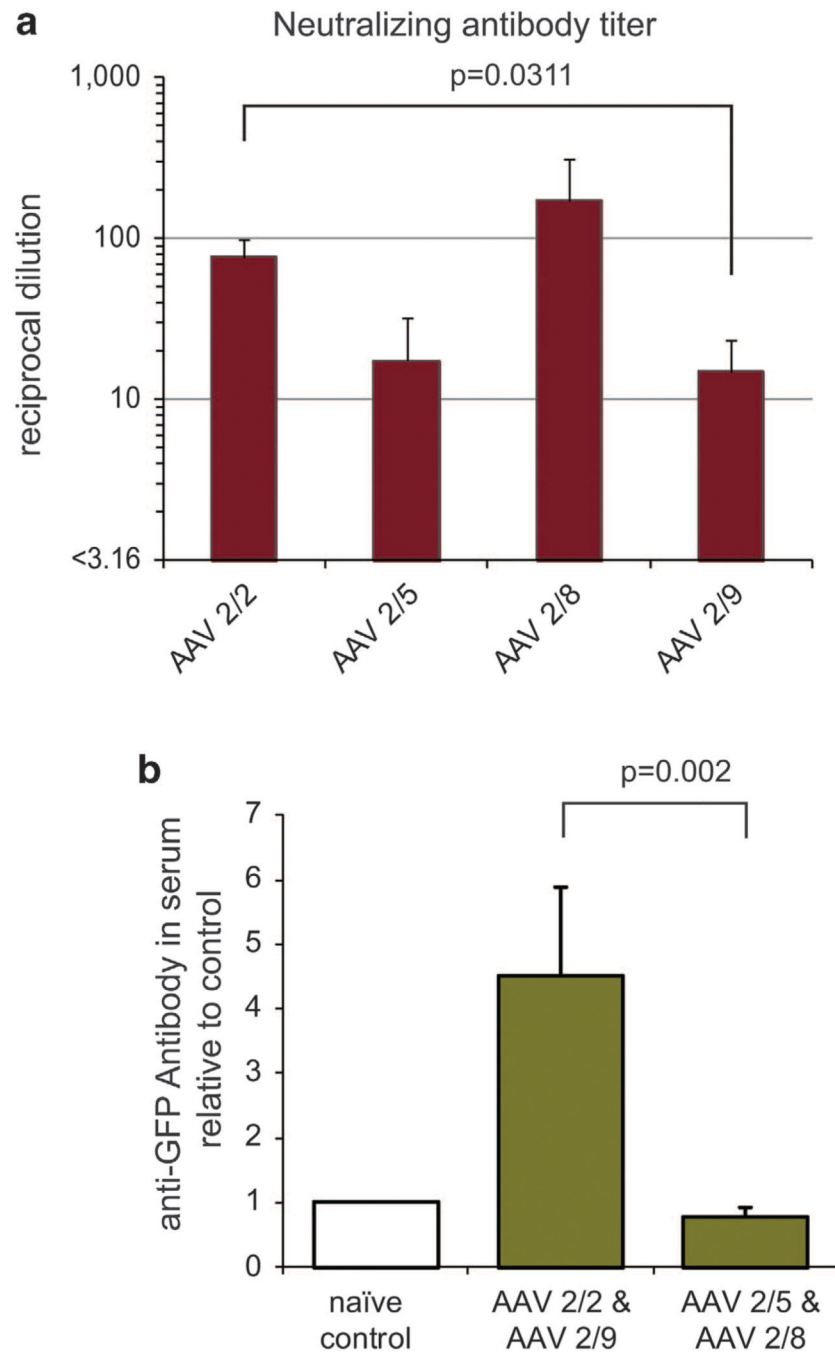


**Figure 5.**

Immune responses to the rAAV serotypes and to GFP. **(a)** Quantification of Nab assay reported as the reciprocal of the most dilute serum concentration that blocked infections (+s.e.m.). Note that the antibody response to rAAV2/2 was significantly greater than that to rAAV2/9, there were no other significant differences. **(b)** Indirect ELISA detecting anti-GFP antibodies in the serum, reported relative to a naïve cat (+s.e.m.). Cats injected with rAAV2/2 and 2/9 showed a significantly higher response to GFP than those injected with

rAAV2/5 and 2/8. Both assays were performed in triplicate. For animals exposed to rAAV2/2 and rAAV2/9,  $n=3$  and for AAV2/5 and rAAV2/8,  $n=2$ !

Author Manuscript

Author Manuscript

Author Manuscript

Author Manuscript

Table 1

Summary of rAAV transduction

Vector	Cat #	Eye #, OS/OD	Concentration	<i>In vivo</i> assessment		Histological assessment		
				Onset of fluorescence (days)	Onset by vector (days; range, mean)	% cones transduced	% rods transduced	Rods versus cones; <i>P</i> , test
rAAV2/2	1	1, OS	$10^{11}$ vgml <sup>-1</sup>	3	3-4, 3.3 (SD = 0.87)	78% (SD = 19)	6% (SD = 3)	<i>P</i> = 0.0033, two-tailed <i>t</i> -test
	2	2, OS	$10^{11}$ vgml <sup>-1</sup>	4				
	3	3, OS	$10^{11}$ vgml <sup>-1</sup>	4, excluded <sup>a</sup>				
	4	4, OS	$10^{11}$ vgml <sup>-1</sup>	Excluded <sup>b</sup>				
rAAV2/5	5	1, OD	$10^{11}$ vgml <sup>-1</sup>	7	4-7, 5.1 (SD = 1.86)	74% (SD = 20)	15% (SD = 13)	<i>P</i> = <0.000, two-tailed <i>t</i> -test
	6	2, OD	$10^{11}$ vgml <sup>-1</sup>	7				
	7	3, OD	$10^{11}$ vgml <sup>-1</sup>	6				
	8	4, OD	$10^{11}$ vgml <sup>-1</sup>	UTD <sup>+</sup>				
	9	5, OD	$10^{11}$ vgml <sup>-1</sup>	4				
	10	6, OD	$10^{11}$ vgml <sup>-1</sup>	4				
rAAV2/8	5	1, OS	$10^{11}$ vgml <sup>-1</sup>	3	1-3, 2.4 (SD = 0.77)	85% (SD = 13)	18% (SD = 25)	<i>P</i> = <0.001, Mann-Whitney rank sum test
	6	2, OS	$10^{11}$ vgml <sup>-1</sup>	2				
	7	3, OS	$10^{11}$ vgml <sup>-1</sup>	1				
	8	4, OS	$10^{11}$ vgml <sup>-1</sup>	3				
	9	5, OS	$10^{11}$ vgml <sup>-1</sup>	3				
	10	6, OS	$10^{11}$ vgml <sup>-1</sup>	2				
rAAV2/9	1	1, OD	$10^{11}$ vgml <sup>-1</sup>	3, excluded <sup>a</sup>	2-3, 2.6 (SD = 0.55)	51% (SD = 13)	4% (SD = 0.6)	<i>P</i> = 0.0028, two-tailed <i>t</i> -test
	2	2, OD	$10^{11}$ vgml <sup>-1</sup>	2				
	3	3, OD	$10^{11}$ vgml <sup>-1</sup>	Excluded <sup>b</sup>				
	4	4, OD	$10^{11}$ vgml <sup>-1</sup>	Excluded <sup>b</sup>				

Key:

<sup>+</sup>UTD: unable to determine; Vitreal hemorrhage precluded fundus examination.<sup>a</sup>Excluded from histological analysis only, because of poor section quality. Please refer to methods for histological assessment procedure.<sup>b</sup>Excluded because of inflammation that developed immediately postoperatively.

**Table 2**

## Feline inner retinal cell transduction

Vector	Antibody			
	Pkc- $\alpha$	GS	Calbindin	Calretinin
rAAV2/2	—	+	—	—
rAAV2/5	—	+	—	—
rAAV2/8	—	+	—	—
rAAV2/9	—	+	—	—

Abbreviations: GS, glutamine synthetase; Pkc- $\alpha$ , protein kinase c- $\alpha$ . Summary of immunohistochemistry results. + sign indicates overlap of the antibody with GFP expression and suggests transduction of the corresponding cell type. All vectors showed Müller cell transduction, as indicated by GS overlap with GFP. No vectors showed bipolar cell transduction or horizontal cell transduction, as indicated by a lack of overlap between GFP and Pkc- $\alpha$ , and calbindin and calretinin.

**Table 3**

Antibodies used for immunohistochemistry

Antibody	Host	Target	Concentration	Source
<i>Primary antibodies</i>				
Cone Arrestin	Rabbit	Cone photoreceptors	1:10 000	Dr Cheryl Craft, Doheny Eye Institute, University of Southern California, Los Angeles, CA, USA <sup>40</sup>
Glutamine Synthetase	Rabbit	Müller cells	1:1000	Sigma Aldrich Inc., St Louis, MO, USA
Glial Fibrillary Acidic Protein	Rabbit	Activated Müller cells	1:1000	DakoCytomation, Carpinteria, CA, USA
Protein kinase c-alpha	Mouse	Rod bipolar cells	1:3000	BD Biosciences, San Jose, CA, USA
Calbindin	Mouse	Horizontal cells	1:1000	Swant Immunochemicals, Bellinzona, Switzerland
Calretinin	Rabbit	Horizontal cells	1:1000	Swant Immunochemicals
GFP	Rabbit	Green fluorescent protein	1:1000	Invitrogen, Carlsbad, CA, USA
<i>Secondary antibodies</i>				
Alexa Fluor 546 F(ab') <sub>2</sub> fragments of goat anti-rabbit IgG (H+L)	Goat	Rabbit primary antibody	1:250	Invitrogen
Alexa Fluor594 rabbit anti-mouse IgG (H+L)	Rabbit	Mouse primary antibody	1:250	Invitrogen



**Table 4**

## Inflammatory infiltration scoring rubric

Ocular region	Scoring system
Retina	Based on thickness of infiltration around blood vessels 0: no infiltration 1: 1–2 cell layers thick 2: 3–4 cell layers thick 3: 5+ cell layers thick
Subretinal space	0: no infiltration 1: scattered individual cells 2: moderate number of cells with some aggregates 3: large numbers of cells causing expansion of the subretinal space
Choroid and episclera	0: no infiltration 1: scattered individual cells 2: moderate number of cells with some aggregates 3: large numbers of cells causing expansion of the choroid space
Ciliary body	0: no infiltration 1: scattered individual cells 2: moderate number of cells with some aggregates 3: large numbers of cells
Total infiltration score sum of all scores above (possible range 0–12)	